SUPERFERRIC RAPIDLY CYCLING MAGNETS OPTIMIZED FIELD DESIGN AND MEASUREMENT *

P. Schnizer†, E. Fischer, H.R. Kieswetter, T. Knapp, T. Mack GSI, Darmstadt, Germany
B. Schnizer, TUG, Graz, Austria
P. Akishin, JINR, Dubna, Russia
R. Kurnyshov, Elektroplant, Moscow, Russia
P. Shcherbakov, IHEP, Protvino, Russia
G. Sikler, W. Walter, BNG, Würzburg, Germany

Abstract

FAIR will feature two superconducting fast ramped synchrotrons. The dipole magnets for one of them, SIS 100, have been designed and full size magnets were built. The properties of the magnetic field were analysed using OPERA (for DC operation) and ANSYS for dynamic calculations. Elliptic multipoles fulfilling the Laplace Equation in plane elliptic coordinates describe the field within the whole aperture consistently within a single expansion. Further circular multipoles, valid within the ellipse, can be calculated analytically from the elliptic multipoles. The advantage of this data representation is illustrated on the FEM calculation performed for SIS 100 dipoles and quadrupoles currently foreseen for the machine.

INTRODUCTION

The Facility of Proton and Iron Research (FAIR) will construct a set of accelerators and storage rings at GSI. The SIS 100 synchrotron, the core component uses superferric magnets, operated at 4 T/s and 1.9 T maximum field. The coil of these magnets use the Nuclotron type cable, where superconducting wires are wrapped around a NiCr tube cooled by a forced two phase Helium flow. The whole concept of the SIS 100 follows the JINR/Nuclotron design, but used the opportunity of the second generation machine to improve various parameters. These include: the loss per magnet, improved field quality and thorough investigation using commercial Finite Element Codes [1]. The first SIS 100 full size dipole was produced last year and is ready for testing (see Fig. 1).

Conventional magnets found in accelerators provide typically a rectangular aperture and for accelerators of small circumference (up to a radius of a few tens of meter) these are also of curved shape. These magnets were typically measured using search coil probes. As these SIS 100 synchrotron magnets are housed in a interconnected cryostat, introducing additional magnetic elements requires to warm up the machine, cut the connections, and reweld them afterwards as well as a cooling them down again. Therefore the field properties have to be fully understood right from the beginning and a sufficently accurate and concise field description is required.

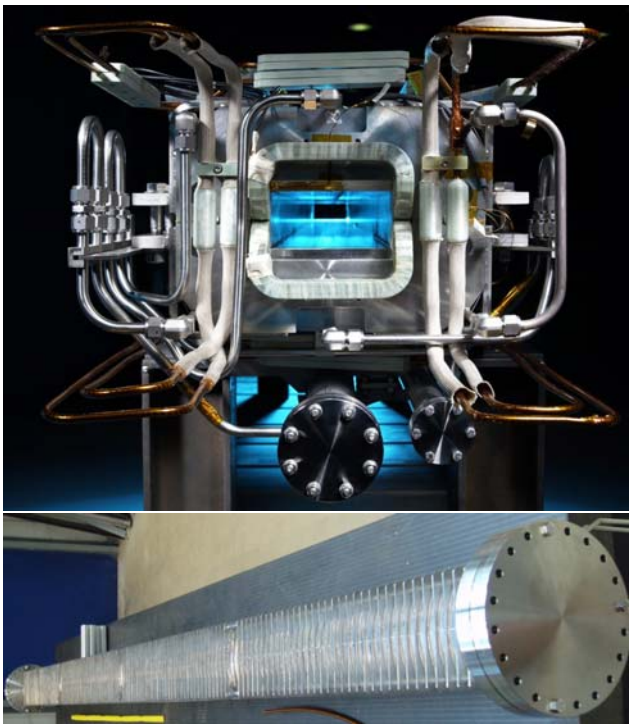

Figure 1: The first SIS 100 full size dipole (top) and the vacuum chamber (bottom).

A common type of such a description is an expansion in plane circular multipoles [2]. We generalized the concept by introducing plane elliptic multipoles [3, 4] as particular solutions of the potential equation in elliptical coordinates. The complete set of basis function needed for an expansion of an arbitrary solution is only a true subset of all these solutions. The advantage is that the reference curve is an ellipse accomodated to the rectangular transverse gap cross section, which covers a larger area than that of a possible reference circle. This expansion prooved to be superior to the circular expansion. A method to extract the elliptic expansion coefficients from experimental data acquired by rotating coils has been proposed and tested numerically[4].

As the SIS 100 dipoles are curved we started to investigate this question by another generalization defining plane

* This work is supported by the EU FP6 Design Study (contract 515873 - DIRAC secondary beams)
† p.schnizer@gsi.de

toroidal multipoles. These are again particular solutions of the potential equation in local toroidal coordinates. With the separation method analytical solutions in these coordinates can be calculated approximately using only power series expansions in the inverse aspect ratio (= the fraction minor/larger radius), cf. eq.(11). This method is well-known in the microwave theory for curved waveguides [5]. The multipole solutions so obtained show very clearly the effects of the curvature and their magnitude, which is of the order of the inverse aspect ratio.

THEORY

The SIS 100 magnets provide an elliptic aperture and the dipoles are curved to follow the beam sagitta. For a thorough understanding of the measurement a solution of $\Delta\Phi = 0$ is required.

Circular Multipoles

The two field components B_x, B_y of a plane irrotational source-free static magnetic field are combined to a complex field $\mathbf{B} := B_y + iB_x$ depending on the complex variable $\mathbf{z} := r\, e^{i\theta}$; they are expanded in circular multipoles

$$\mathbf{B} = \sum_{m=0}^{M} \mathbf{C}_m\, (r/R_{Ref})^m\, e^{im\theta} \quad (1)$$

$$\mathbf{C}_m = \frac{1}{2\pi}\int_{-\pi}^{\pi} \mathbf{B}(\mathbf{z} = R_{Ref}\, e^{-im\theta})\, e^{-im\theta} d\theta, \quad (2)$$

with M the number of multipoles used. The expansion coefficients may be computed from field values given along the reference circle $r = R_{Ref}$ as indicated in eq.(2). The US notation is used within this paper (0 ... dipole, 1 ... quadrupole, ...) as the following calculations are then more straight forward. The coefficients $\mathbf{C}_m$ can be recalculated using

$$b_n + ia_n = \mathbf{c_n} = \mathbf{C_m}/\mathbf{C_{main}} \quad (3)$$

with C_{main} the main harmonic of the magnet. The b_n's and a_n's are dimensionless constants.

Elliptic Multipoles

A reference ellipse with semi-axes $a > b$ accomodated to a rechtangular gap covers a larger domain than a reference circle of radius R_{Ref}. The excentricity e specifies the corresponding elliptic coordinates η, ψ, [6, 4, 3]

$$x = e\cosh\eta\cos\psi, \quad 0 \le \eta \le \eta_0 < \infty; \quad (4)$$

$$y = e\sinh\eta\sin\psi, \quad -\pi \le \psi \le \pi. \quad (5)$$

$\eta_0 = \tanh^{-1}(b/a)$ gives the reference ellipse. A plane irrotational source-free field is expanded w.r.t. the complete system of elliptic multipoles as

$$\mathbf{B} = \sum_{n=0}^{M} \mathbf{E}_n\, \cosh[n(\eta + i\psi)]/\cosh(n\eta_0),$$

$$\mathbf{E}_n = \frac{1}{\pi}\int_{-\pi}^{\pi} \mathbf{B}(\mathbf{z} = e\cosh(\eta_0 + i\psi))\, \cos(n\psi)\, d\psi. \quad (6)$$

The expansion coefficients $\mathbf{E}_n$ may be computed from field values given along the reference ellipse (6).

The two sets of expansion coefficients belonging to the same $\mathbf{B}$ may be converted to each other using

$$\mathbf{E}_n/\cosh(n\eta_0) = \sum_{m=0}^{M} \mathbf{C}_m\, \beta^m\, d_{mn}, \quad (7)$$

$$2\,\mathbf{C}_m\, \beta^m = \sum_{n=0}^{M} \mathbf{E}_n/\cosh(n\eta_0)\, c_{nm} \quad (8)$$

with $\beta := e/(2R_{Ref})$. The transformation matrices $D = (d_{mn})$ and $C = (c_{nm}) = D^{-1}$ are given by

$$d_{mn} = [1 + (-1)^{m+k}] \begin{pmatrix} m \\ (m-k)/2 \end{pmatrix}. \quad (9)$$

The elements of C may be found by symbolic or numeric inversion of D; closed expressions have been given elsewhere [3]; in [7] they are computed by recurrences. In this paper the coefficients b_n and a_n are given in units i.e. $1\,unit = 100\,ppm$ at a R_{Ref} of $40\,mm$. We chose this free parameter such that the relative allowed harmonics b_n can then be represented as convenient numbers in the order of 1 to 10. Using (6) the field can be interpolated with sufficient accuracy within an ellipse with half axes a, b.

Toroidal Multipoles

In a curved magnet a torus segment ($|\varphi| \le \varphi_0$) is introduced as a reference volume. Dimensionless local toroidal coordinates are defined by

$$X + iY = R_C\, h\, e^{i\varphi},\ Z = R_{Ref}\sin\vartheta,\ h = 1 + \epsilon\rho\cos\vartheta. \quad (10)$$

R_{Ref} (R_C) are the minor (major) radii of the torus.

$$\epsilon := R_{Ref}/R_C \quad (11)$$

is the inverse aspect ratio, on which the curvature effects depends. As $\epsilon << 1$ working with power series in ϵ is a useful approximation scheme. The centre of the fundamental Cartesian system (X, Y, Z) coincides with that of the torus, Z is normal to the equatorial plane. The quasi-radius $R_{Ref} \cdot \rho$, $0 \le \rho \le 1$, is the normal distance of the field point from the centre circle; the poloidal angle $-\pi \le \vartheta \le \pi$, is around the centre circle; the toroidal angle $-\pi \le \varphi \le \pi$ agrees with the common azimuth, cf. [8], [5]. Only toroidally uniform fields are considered; their field components B_ρ, B_θ are confined to the planes φ = const. and are independent of φ.

The potential equation independent of φ is solved by an approximate R-separation. Thus the approximate multipole solution for the potential is (m = integer)

$$\Phi_m = \rho^{|m|}\, e^{im\vartheta} - \frac{\epsilon}{4}\,\rho^{|m|+1}\big(e^{i(m+1)\vartheta} + e^{i(m-1)\vartheta}\big) + O(\epsilon^2). \quad (12)$$

So the curvature adds just the two adjacent multipoles; the magnitude of these admixture is not larger than $\epsilon/2$. Expressions for the corresponding magnetic fields have been derived as well as their orthogonality relations. This permits us to give the field expansion w.r.t. the basis fields and to calculate the expansion coefficients for a field given along the reference circle. A report will be published.

Tests

The formulae described above were used to analyse all the magnet data calculated for the SIS 100 main magnet designs. The field quality was calculated for the **C**urved **S**ingle **L**ayer **D**ipole with **8** turns [4, 9, 10, 11], the dipole design chosen for the main dipole for the SIS 100 machine of FAIR. The field quality of this magnet is calculated by

$$\mathbf{\Delta B(z)} = (\mathbf{B(z)} - \mathbf{B(0)}/\,\mathbf{B(0)} \cdot\ 10^4\,. \qquad (13)$$

They are now applied to fields to demonstrate that all these steps are necessary to interpolate the field within the ellipse with a precision of better than the maximum tolerable field deviation of 600 ppm or 6 units (1 unit corresponds to 100 ppm). The original distribution is given in Fig. 2(a) at a current of $873kA$ yielding a field of $\approx\ 0.13T$. The field was taken along the ellipse and the elliptic multipoles were calculated as defined in (6). Using the first 20 coefficients the field was interpolated within the aperture (see Fig. 2(b)). The naked eye can not see any difference to the original data (Fig. 2(a)). The original field was subtracted from the interpolated one. One can see from Fig. 2(c) that this difference is well below half a unit and thus sufficiently precise. Normally circular multipoles are used. So we calculated them using a Fourier Transform of the data along a circle. Again the interpolation data was calculated (see Fig. 2(g)) and the difference to the original data (see Fig. 2(d)) using the first 15 coefficients. One can see that the interpolation works well within the circle but outside the circle soon the errors get unacceptably large. The difference outside of the circle is even larger if more coefficients are used. At last the circular multipoles were calculated from the elliptic ones as described in (9) (see Fig. 2(e) for the interpolation and Fig. 2(f)) for the difference). One can see that contrary to the circular interpolation, this interpolation works even outside the circle and within the whole ellipse.

PRODUCTION REVIEW

The magnetic field quality is defined by the yokes geometry (in the centre) and by the yokes end shape and the coils' position (in the ends). Thus all magnets (108 dipoles) must match each other and the temporal evolution of their field on each cycle. This will be guarantied by a very reliable mechanical fixture of the superconducting cable, especially in the head parts of the coil.

A cable machine was dedicated to produce the Nuclotron-type cable, which was optimised to guarantee and maintain constant cable parameters. This cable is wound to half coils of $4 \cdot 2$ windings in two layers and is supported by a precisely machined surrounding mechanical fixture made of glass-fibre reinforced plastic (GRP). The poles are finally shaped in a combined heat pressure treatment with an accuracy of the outside dimensions $< 0.05mm$ (also in the coil ends) and thus the superconducting wires positions is predominantly defined by the manufacturing tolerances of the GRP structural elements ($< 0.1mm$).

The soft-magnetic iron yoke of this dipole is made of two half shells which are bolted together. This allows to insert and remove the beam pipe and the coils. The yoke laminations are of "electrical sheet metal" with a thickness of 1 mm. They were laser-cut and stacked to sub-packs of approximately 150 mm length. The laminations were covered with adhesive which is activated and hardening when heated. The sub-packs are glued together in a furnace under pressure to form a solid compound for further assembly. Each of these packs show a packing factor of 99.5 %. (Smaller packing factors can be reached controlling the pressure during the backing process). The sub-packs are set up in a string along with the two specially shaped end-packs and a compensating pack to reach the required magnet length. On the outside corners of the yoke cooling tubes and angular sheets of stainless steel are placed. The stainless steel- angels form an outside frame for the yoke. They are TIG-welded at various positions to each sub-pack along the whole length of the yoke. The heat introduced during the welding process can distort the shape, thus the welding pattern was optimised to keep the distortion small and the evenness of the relevant yoke surfaces within the tolerance of 0.3 mm (over the whole length of 2.8m).

EXPECTED FIELD QUALITY

Static

Many different models were built and investigated in 2 and 3 dimensions to obtain a magnetic field design providing a field quality according to the specifications. The design to prefer was chosen based on the circular multipoles calculated from the elliptic ones. A side to that the influence of the packing factor was studied for the dipole as foreseen for SIS 100 (see Fig. 3, gap height was 66 mm for this study). One can see that the influence of the packing factor on the field quality is rather small up to a field of $\approx 2.1\,T$ (roughly half a unit for b_3 and 0.1 unit for b_5) and less than 0.1 units at injection.

Dynamic

As the SIS 100 machine is designed to run with an frequency of roughly 1 Hz, the dipole magnets must be ramped from the injection field of $\approx\ 0.23\,T$ to $\approx\ 1.9\,T$ in the order of half a second. The ramping field generates eddy currents in different parts of the magnet [1] and also in the vacuum chamber [12]. The same model as in [12] was used again to calculate the magnetic field using AN-

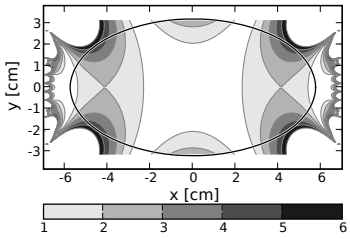

(a) Deviation of original data from a pure dipole field

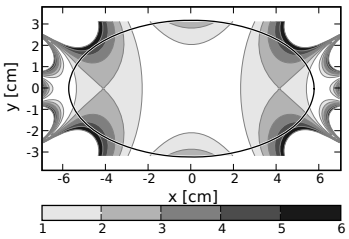

(b) Deviation of field computed by elliptic expansion from dipole field

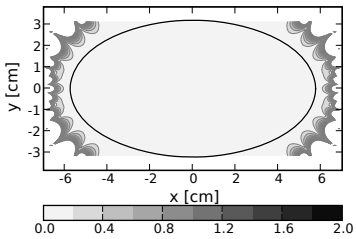

(c) Difference between original field data and those computed by elliptic expansion

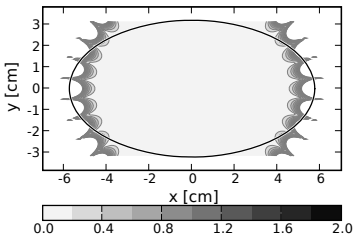

(d) Difference between original field data and those computed by circular expansion

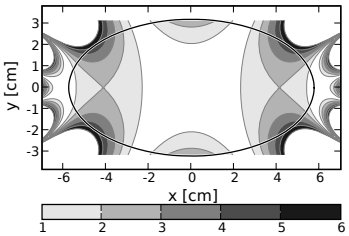

(e) Deviation of field computed by circular expansion with circular coefficients converted from elliptic coefficients, eq.(9)

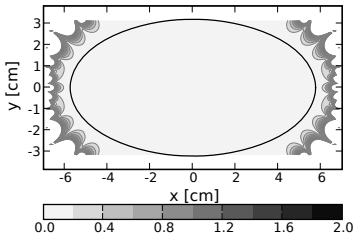

(f) Deviation of original field data from data computed as described at left

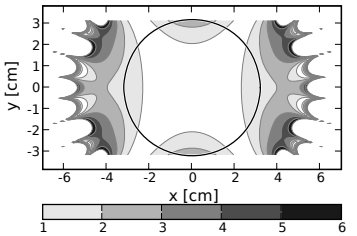

(g) Deviation of field computed by circular expansion from dipole field

Figure 2: Test of the interpolation for the CSLD8b at a current of $873\,kA$ and a field of $\approx 0.13\,T$. The field B_y in the aperture is plotted. The gray indicates the absolute value of the deviation (in units). The original data are given on top. The upper row shows the data as reconstructed using the interpolation and the lower columns shows the absolute value of the difference between the reconstructed and the original data.

SYS (see Fig. 4) in the "2D" section of the magnet. The model was evaluated for static operation without the vacuum chamber, for static operation with the vacuum chamber and for the dynamic operation with the vacuum chamber (see Fig. 5 to Fig. 8). One can see that the field does not change in the longitudinal position, but that at injection the eddy currents create a distortion at least twice larger than the field the magnet provides (see also Fig. 9). At intermediate field levels (see Fig. 6) the relative contribution of the eddy currents is comparable to the static ones. Above 1.8 Tesla the iron starts to saturate. Thus the field quality is dominated by saturation levels above this value. The elliptic multipoles and the circular ones derived from the elliptic ones [3, 13] were calculated and the field was reconstructed using them. Fig. 9 demonstrates that the interpolation represents the original field with sufficient accuracy. The multipoles along the load line on the ramp up are given in Fig. 10.

One can see that the vacuum chamber adds the largest distortion at the injection field level, as the effect only depends on $\mathrm{d}B/\mathrm{d}t$ and thus is constant for constant ramp rate, whereas the other artefacts contributions increase with increasing field level.

MEASUREMENT

Rotating Coils in Elliptic apertures

Search coils are normally used to measure dipoles with rectangular apertures. These, however, are useful instruments when they can be moved on perfectly machined surfaces (e.g. pole shoes). Rotating coils have been proposed as a work horse for measuring the synchrotrons at GSI, as

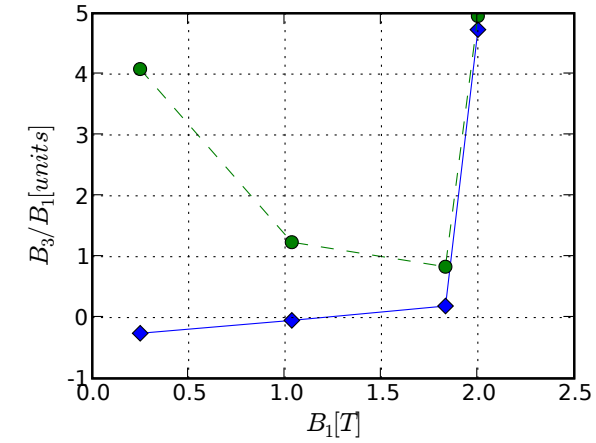

(a) b_2

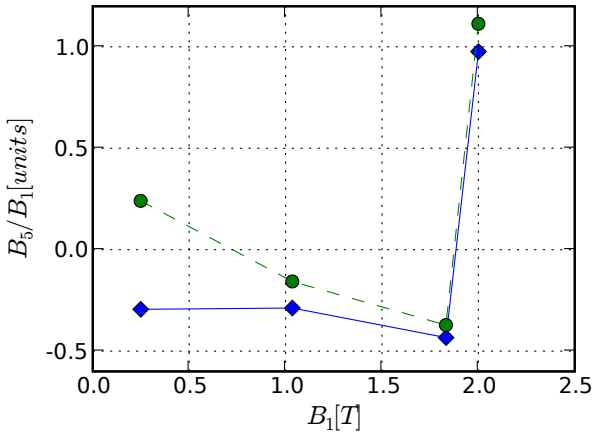

(b) b_4

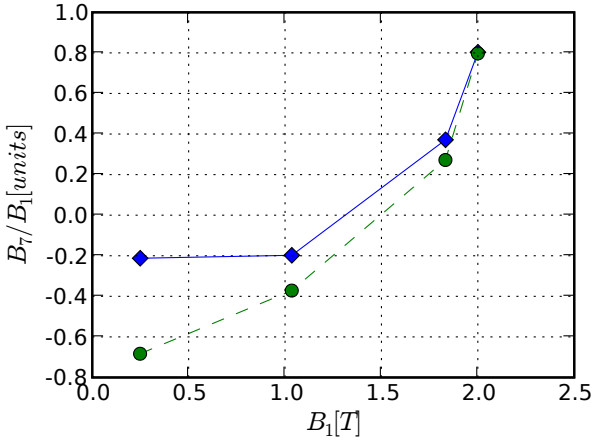

(c) b_6

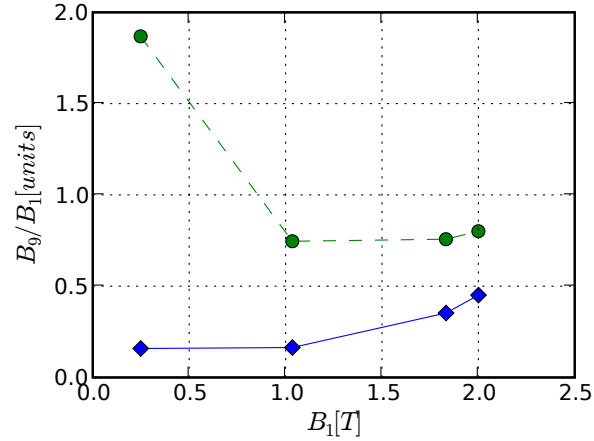

(d) b_8

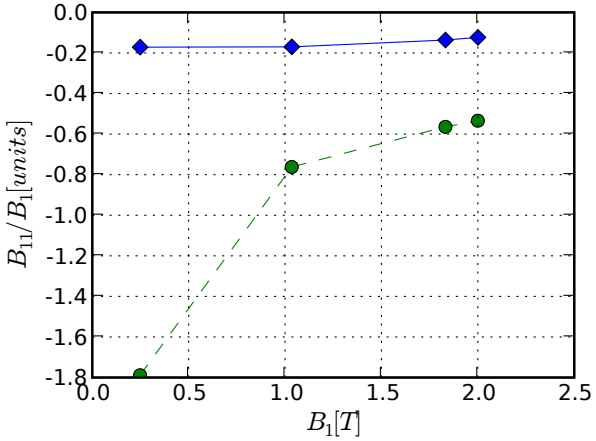

(e) b_{10}

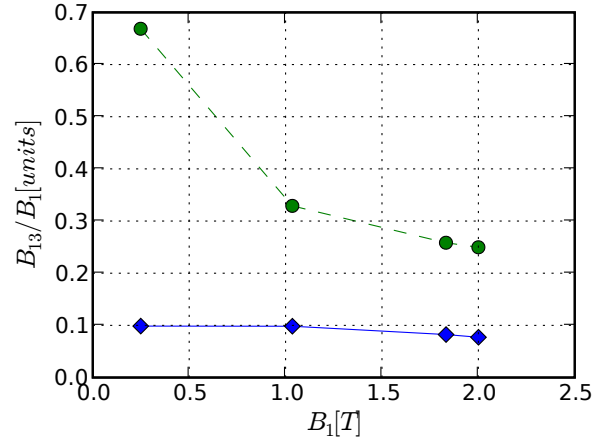

(f) b_{12}

Figure 10: The field quality for the BNG magnet. The solid blue line represents the **static** field **without** vacuum chamber, the green dashed line represents the **dynamic** field **with** vacuum chamber at a ramp rate of $\approx 4\,T/s$. One can see that at injection the field is considerably distorted due to eddy current effects.

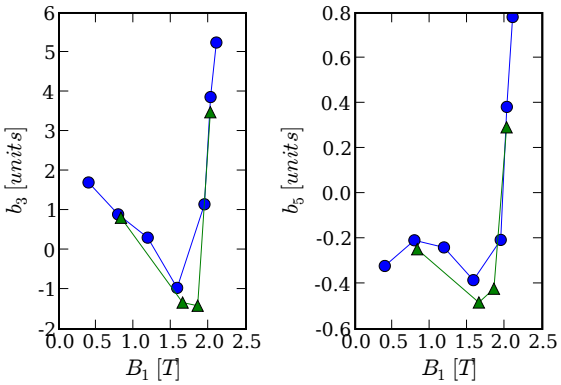

Figure 3: Relative 2D harmonics of the static field quality versus the main field for different packing factors (circles 98 %, tripods 100 %). The difference between the lines is not large compared to a maximum tolerable field error of 6 units.

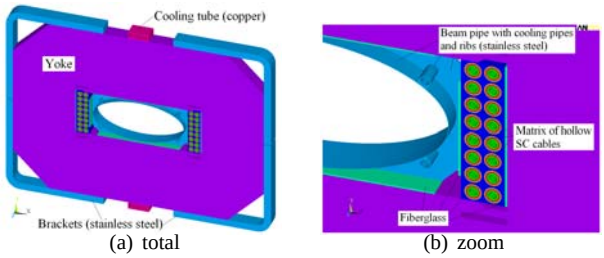

(a) total (b) zoom

Figure 4: The model of the middle section of the dipole magnet and the vacuum chamber. The vacuum chamber is supported by ribs and equiped with separate cooling tubes.

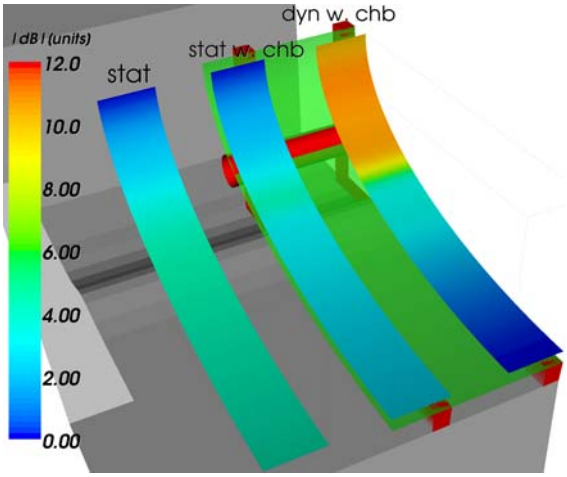

Figure 5: The field deviation in units (1 unit = 100 ppm) at injection is plotted along the ellipse. left → the static field without vacuum chamber, middle → static field with the vacuum chamber, right → the dynamic field with the vacuum chamber. The quater yoke is indicated in gray, the vacuum chamber in green and in red the supporting ribs and cooling tube. The eddy currents create the main distortion.

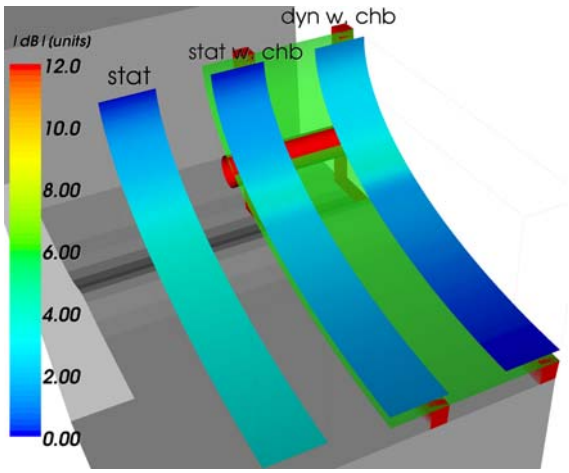

Figure 6: The field quality at a current of roughly $1.04T$ at a time of $250\,ms$. The maximum deviation is about 5 units for all, but the dynamic one has a higher variation (i.e. additional multipoles)

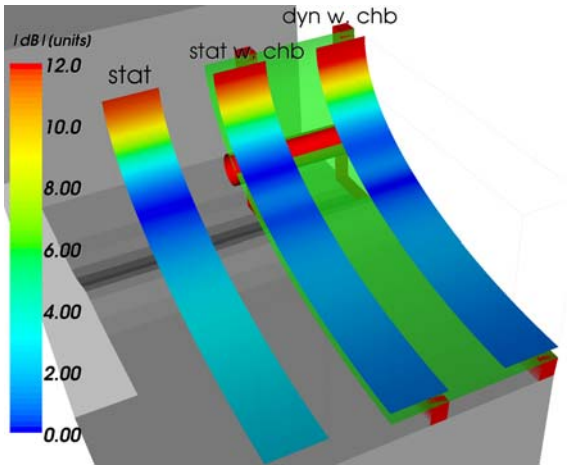

Figure 7: The field quality at a current of roughly $1.832T$ at a time of $450\,ms$. One can see that the saturation is the main reason for the field detioriation, but the eddy currents generate higher order multipoles and it is a factor 3 (dynamic case) to 10 (static case) higher than at injection.

they provide the field within their rotation radius. This does not cover the whole aperture, and thus they must be placed laterally at different positions. The measurements can then be used to calculate the field on the ellipse using appropriate weights for the different measurements [4]. The circular multipoles are then calculated as described by (9).

Ramping field

Rotating coils are typically operated at rotation speeds of roughly one revolution per second measuring the flux at different angular position ($\approx$ 100 positions). This approach is not appropriate for SIS 100, as the machine cycle time is also in the order of one second. Therefore the "step by step" method is used. Here the coil probe is placed at some

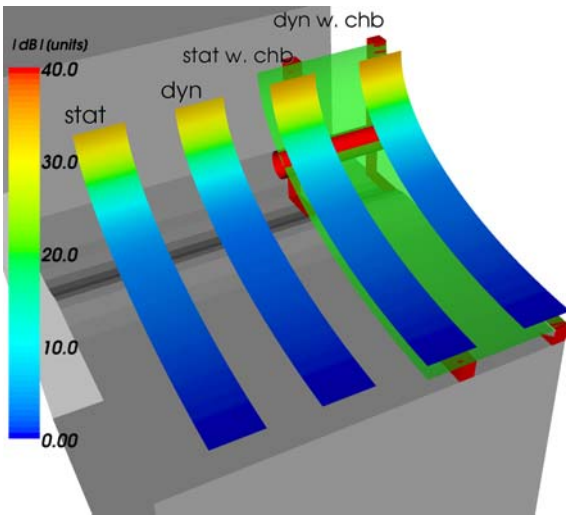

Figure 8: The field quality at a current of roughly $2.00T$ at a time of $500\,ms$. The field quality in mainly determined by the saturation of the iron. The effect of the vaccuum chamber and the effect of the eddy currents does not contribute significantly.

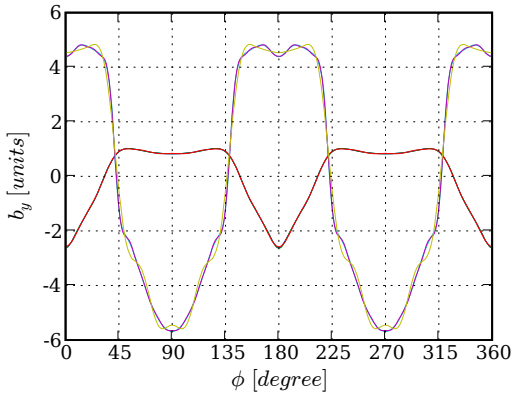

Figure 9: The field B_y at injection versus the angle ϕ around the ellipse. The static field (variation $\approx$ 2 units) versus the dynamic field (variation $\approx$ 10 units). The data calculated with ANSYS are plotted next to the interpolation using the elliptic multipoles and the circular multipoles derived from the elliptic ones.

start angle θ_0. The magnet is then pulsed once and the field is measured. Then the coil is advanced by some angle $\delta\theta = 2\pi/m$. The magnet is pulsed again and the field measured. This is performed until the start angle is reached again. Now the data of the different pulses are resorted for each point in time, and then the multipoles are calculated [14].

Using a "compensating coil probe array", which suppresses the voltage induced by the main harmonic by a factor of 100 – 1000, one can not only reduces the required electronics accuracy but also reduces the artifacts created by angular positioning errors on higher order harmonics. This approach was tested on the magnet "GSI 001" using a simple test setup and comparing the results to the measurements obtained by A. Jain at BNL [15].

CONCLUSION

The first SIS 100 full size dipole has been delivered and is made ready for testing at GSI. Elliptic multipole expansions for a plane irrotational, source-free, static magnetic field were demonstrated in a domain bounded by an ellipse as reference curve similar as for circular multipoles within a circle. In both cases the expansion coefficients of the complex field can be computed from the field given along the reference curve. The ellipse covers a larger area in the gap and thus the convergence properties are better for the elliptic expansion. The calculated static and dynamic field quality were presented. The 2D static field quality is mainly determined by the imperfections of the magnets geometry whereas the dynamic field quality is considerably affected by the eddy currents in the vacuum chamber. This magnet will be tested this summer, measured magnetically and the results presented here will be checked with the measurement data. A second full size dipole is under construction at JINR / Dubna and will be tested there soon and afterwards retested at GSI [16].

REFERENCES

[1] E. Fischer, R. Kurnishov, and Shcherbakov P., "Finite element calculations on detailed 3D models for the superferric main magnets of the FAIR SIS100 synchrotron", *Cryogenics*, 47:583–594, 2007.

[2] A. K. Jain, "Basic theory of magnets". CERN 98-05, European Organization for Nuclear Research, Geneva 1998. pp.1 - 26.

[3] P. Schnizer, B. Schnizer, P. Akishin, E. Fischer, "Field representations for elliptic apertures" February 8th, 2007. GSI Internal Communication. Revised January 16th, 2008.

[4] P. Schnizer, B. Schnizer, P. Akishin, E. Fischer, "Magnetic field analysis for supperferric accelerator magnets using elliptic multipoles and its advantages". 20-th Magnet Technology Conference, August 27-30, 2007, Philadelphia, Pa., USA IEEE Trans. on Applied Superconductivity, Volume 18 , 2008

[5] L. Lewin, D.C. Chang, E.F. Kuester, Electromagnetic Waves and Curved Structures. IEE Electromagnetic wave series 2, 1977.

[6] P. Moon, D. E. Spencer, Field theory handbook: Including coordinate systems, differential equations and their solutions. Springer, 1988. pp. 112 - 115, Fig.4.04.

[7] F. R. Peña and G. Franchetti, Elliptic and circular representation of the magnetic field for SIS 100. GSI Acc-Note-2008.

[8] W.D. D'haeseleer, W.N.G. Hitchon, J.D. Callen, J.L. Shohet, Flux coordinates and magnetic field structure. Springer, 1990.

[9] E. Fischer, H. G. Khodzhibagiyan, "SIS 100 dipole alternatives" Technical Report, GSI, 2007

[10] E. Fischer, H. G. Khodzhibagiyan, A. D. Kovalenko, "Full Size Model Magnets for the FAIR SIS 100 Synchrotron" 20-th Magnet Technology Conference, August 27-30, 2007, Philadelphia, Pa., USA IEEE Trans. on Applied Superconductivity, Volume 18, 2008

[11] P. Akishin, E. Fischer, P. Schnizer, "A single layer dipole for SIS 100", Technical Report, GSI, July 2007

[12] E. Fischer, R. Kurnyshov, and P. Shcherbakov, "Analysis of coupled electromagnetic-thermal effects in superconducting accelerator magnets", In *8^{th} European Conference On Applied Superconductivity, 16 - 20 September 2007, Brussels, Belgium*, volume 97. IOP Journal of Physics: Conference Series, 2008.

[13] P. Schnizer, B. Schnizer, P. Akishin, and E. Fischer, "Theoretical Field Analysis for Superferric Accelerator Magnets Using Elliptic Multipoles and its Advantages" Presented at 12^{th} European Particle Accelerator Conference, Genova, 2008

[14] P. Schnizer et. al "A mole for measuring pulsed superconducting magnets" 20-th Magnet Technology Conference, August 27-30, 2007, Philadelphia, Pa., USA IEEE Trans. on Applied Superconductivity, Volume 18, 2008

[15] A. Jain, G. Ganetis, W. Louie, A. Marone, R. Thomas, and P. Wanderer, "Field quality measurements at high ramp rates in a prototype dipole for the FAIR project," 20-th Magnet Technology Conference, August 27-30, 2007, Philadelphia, Pa., USA IEEE Trans. on Applied Superconductivity, Volume 18, 2008

[16] A. D. Kovalenko et. al, "Full size model magnets for heavy ion superconducting synchrotron SIS100 at GSI: status of manufacturing and test at JINR", Presented at 12^{th} European Particle Accelerator Conference, Genova, 2008